

LBL--33106

DE93 007714

**Magnetic Thin Films and Nanostructures:  
Anisotropy, Microstructure and Their Inter-Relationship**

**K.M. Krishnan**

**Materials Science Division  
National Center for Electron Microscopy  
Lawrence Berkeley Laboratory  
University of California, Berkeley, CA 94720**

**Microstructures of Materials Conference  
22, 23 October 1992**

This work was supported in part by the Director, Office of Energy Research, Office of Basic Energy Sciences, Materials Science Division of the U.S. Department of Energy under Contract No. DE-AC03-76SF00098.

**MASTER**

**DISTRIBUTION OF THIS DOCUMENT IS UNLIMITED**

# Magnetic thin films and nanostructures: Anisotropy, microstructure and their inter-relationship

Kannan M. Krishnan

Materials Sciences Division  
Lawrence Berkeley Laboratory  
University of California, Berkeley, CA 94720

## *Abstract*

Magnetic thin films and nanostructure exhibit novel properties and have great technological potential. In particular, developing thin film structures with perpendicular anisotropy, understanding the underlying mechanisms and identifying meaningful microstructure-property relationships in such nanometer scale materials is an ongoing challenge. Here, two different approaches as well as details of the relevant microstructure are presented.

## I. INTRODUCTION

There has been a recent upsurge of scientific interest in surface, interface and thin film magnetism largely because of the ability to atomically synthesize such materials [1]. In particular, for a ferromagnetic thin film the anisotropy energy includes contributions from surface or interface anisotropy, volume magnetocrystalline anisotropy and the demagnetizing field or shape anisotropy. For thick films ( $\sim$  few nm for transition metals), the demagnetizing field is predominant and the magnetization lies in the plane of the film. For

ultrathin films and multilayers ( $t_m > 1$  nm) the surface/interface contribution, proportional to  $t_m^{-1}$ , can overcome the shape anisotropy and result in a spontaneous magnetization perpendicular to the film. Alternatively, the magnetocrystalline anisotropy can dominate provided the material exhibits strong uniaxial anisotropy and is grown such that the easy axis is oriented along the film normal. From a technological perspective, perpendicular anisotropy lends itself to orders of magnitude increase in magnetic/magneto-optic recording density and epitaxial growth on appropriate substrates could lead to novel magnetic/semiconductor/optical device integration.

In this paper highlights of our research program on both thin films and atomic-scale multilayered nanostructures are discussed. Emphasis is on the evolution and control of microstructures as well as the relationship of the latter to anisotropy mechanisms in such materials.

## II. NEW FERROMAGNETIC THIN FILMS WITH PERPENDICULAR ANISOTROPY

We predict that perpendicular anisotropy in thin films can be achieved by carefully selecting a ferromagnetic material that in the bulk exhibits uniaxial anisotropy (in addition to the right combination of  $T_C$ ,  $H_C$  and saturation magnetization), and grow it epitaxially (good lattice

---

This work was supported by the Director, Office of Energy Research, Office of Basic Energy Sciences, Materials Sciences Division of the US Department of Energy under contract No. DE-AC03-76SF00098. It is also a pleasure to acknowledge Drs. N-H. Cho, B. Zhang, R. Farrow, C. Lucas and Mr. C.J. Echer for their contribution to this research program.

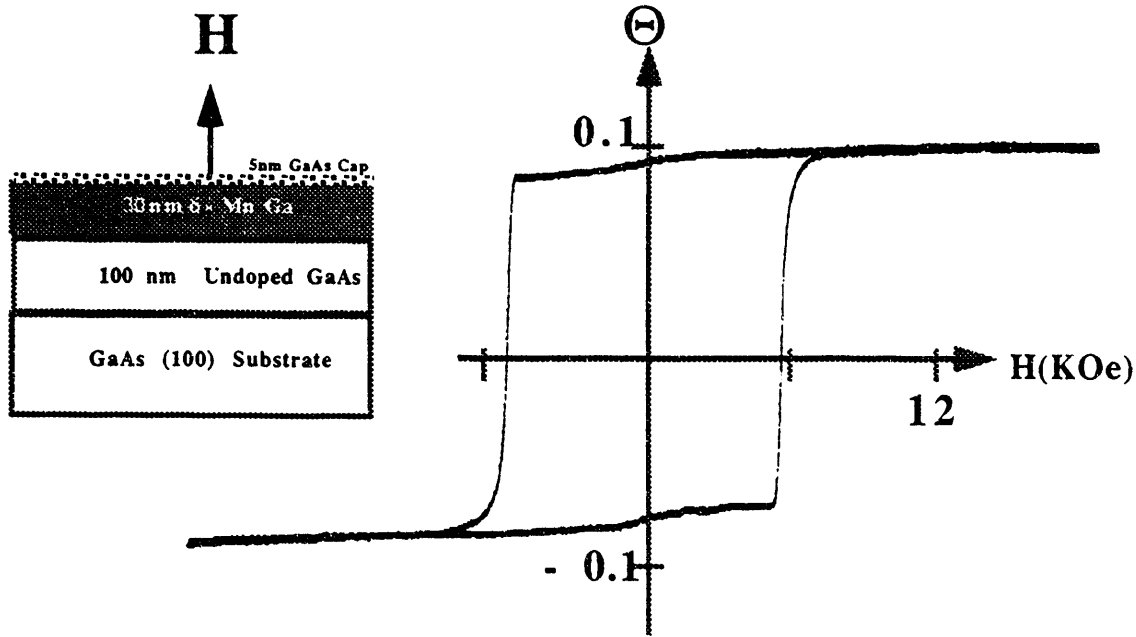


Figure 1: Polar Kerr rotation data for the newly synthesized ferromagnetic thin films . A square loop indicative of perpendicular anisotropy is observed. Contents of the thin film structure and the applied field direction are also shown.

matching is important) on appropriate substrates (preferably on semiconductors for device integration) such that the magnetization is along the film normal. Moreover, the phase of interest should be thermodynamically stable in the bulk, and inter-diffusion as well as interface reactions should be a minimum.

From a detailed evaluation of a variety of materials we concluded that  $Mn_xGa_{1-x}$   $x = 0.6 \pm 0.05$  is the most promising candidate to achieve these stringent mix of properties. In the bulk it is tetragonal (  $a = 2.75 \text{ \AA}$ ,  $c = 3.542 \text{ \AA}$  ) and ferromagnetic (  $H_C(77K) = 1.15 - 4.9 \text{ kOe}$ ,  $T_C = 658-748 \text{ K}$ ,  $\sigma_S(77K, 10kOe) = 48 - 31 \text{ G cm}^3/g$  ) [7]. In addition, growth of the c-axis oriented film on a GaAs (100) substrate ( $a = 5.65 \text{ \AA}$ ) for device integration would be both chemically and crystallographically favourable.

Thin films with a composition  $Mn_{1-x}Ga_x$  ( $x = 0.4$ ) were grown by molecular beam epitaxy. The growth was initiated with a 1nm template at  $20 \text{ }^\circ\text{C}$  followed by continuous deposition at a rate of

$11.5 \text{ \AA}/\text{min}$  at  $100 \text{ }^\circ\text{C}$  upto a thickness of  $300 \text{ \AA}$ . The film was then annealed at  $240 \text{ }^\circ\text{C}$  for 1 min following which a  $50 \text{ \AA}$  GaAs capping layer was deposited.  $\Theta-2\Theta$  scans and corresponding rocking measurements with the film normal in the scattering plane gave  $c = 3.515 \text{ \AA}$  and a spread of the (002)  $Mn_xGa_{1-x}$  peak of about 2.0 degrees. Grazing incident x-ray diffraction measurements, with the film normal perpendicular to the scattering plane, gave an in-plane lattice spacing  $a = 2.79 \text{ \AA}$  and the corresponding  $\phi$  scans reveal an in-plane order of 0.5 degrees. It is clear that the unit cell of this phase is tetragonal and grows with good epitaxy such that the c-axis is oriented normal to the {001} GaAs substrate surface. X-ray emission spectroscopy confirmed the composition to be  $62 \pm 2 \%$  Mn. Polar Kerr rotation, SQUID and vibrating sample magnetometer measurements with the field applied along the thin film normal showed nearly perfect square hysteresis loops confirming perpendicular anisotropy of the films. The film exhibits a Kerr rotation angle of  $\sim 0.1$  degrees at  $820$

nm (figure 1), a coercivity of 6.27 kOe and a saturation magnetization of 460 emu/cm<sup>3</sup>. The optical reflectivity of the film was 65-70% over a broad range of wavelengths. This unique set of properties make it a very promising material [2] for magneto-optic recording with the additional potential of integrating semiconductor/magnetic devices by suitable patterning techniques .

### III. EVOLUTION AND CONTROL OF ULTRATHIN MULTILAYER MICROSTRUCTURES

Nanostructured multilayers can also be made to exhibit perpendicular anisotropy by exploiting their surface and interface properties. However, the origin of perpendicular anisotropy in these materials is poorly understood. Our investigations, including atomic scale synthesis and

characterization, indicates that these magnetic properties can be interpreted in terms of the evolution and control of their complex microstructure. Our discussion is restricted to  $[\text{Co}_x(\text{\AA})\text{Pt}_y(\text{\AA})]_n$ , where  $n$  is the number of repeats, grown on GaAs (111) substrates with or without a Ag buffer layer.

1. *Effect of Ag buffer layer:* Multilayer stacks ( $x=3, y=15, n=15$ ) grown on a 200Å silver buffer layer show strong uniaxial magnetic anisotropy perpendicular to the surface whilst direct growth on GaAs resulted in a predominant in-plane component. Structural measurements by transmission electron diffraction (TED), high resolution electron microscopy (HREM) and x-ray scattering ( $\Theta-2\Theta$  and related rocking scans) confirmed that the deposition of a Ag layer enhances the crystalline quality of the multilayers

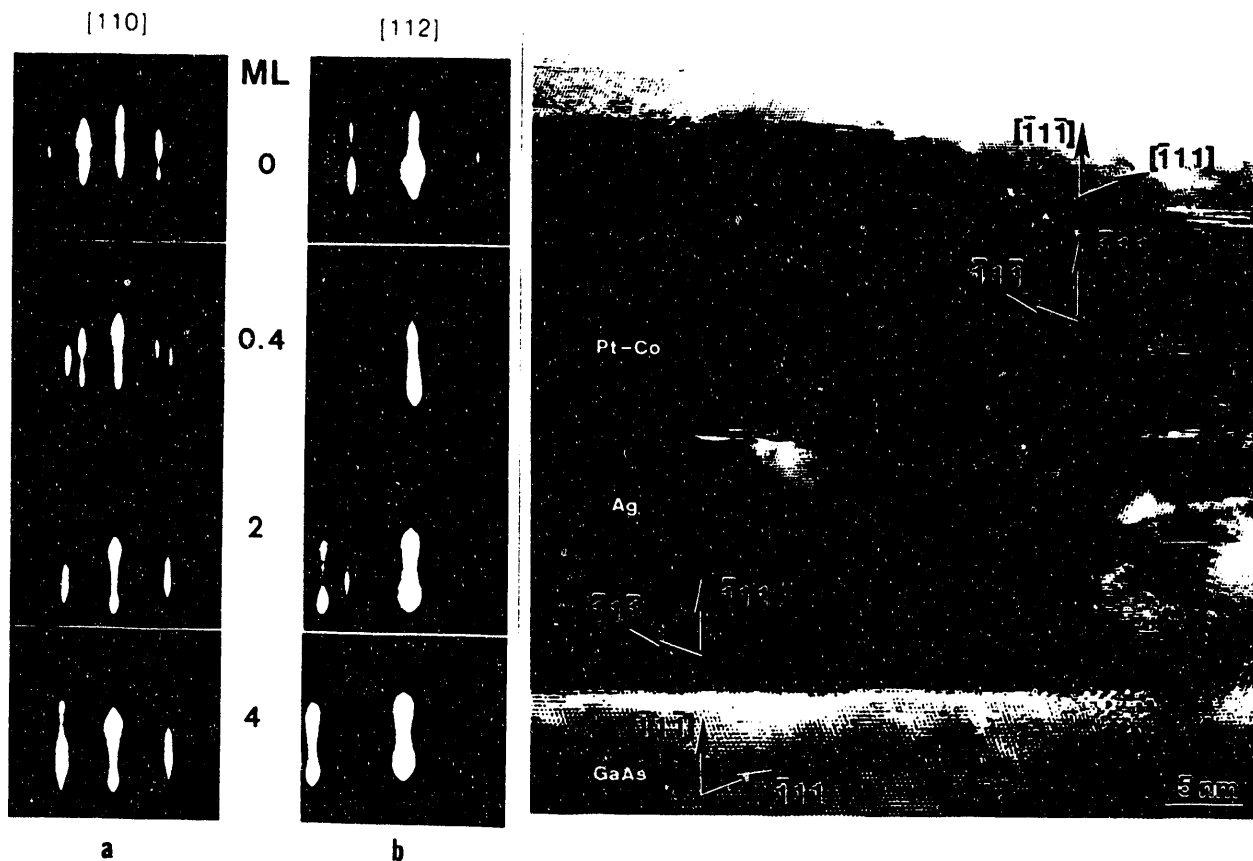


Figure 2: RHEED data from the early stages of growth of the multilayer stack. The same pattern was reproduced when the sample was rotated by sixty degrees. Atomic resolution image of a cross-sectional sample showing the complicated microstructure. The Ag buffer layer stabilizes the nanostructure.

and leads to better epitaxy. Randomly oriented polycrystalline grains, observed for direct growth on GaAs, is thus avoided and a strong (111) texture is achieved [3].

2. *Twin formation and propagation:* In spite of the excellent epitaxy and strong (111) texture, samples grown on a Ag buffer are polycrystalline (in bright field images) with an average grain size of 30-40 nm. For fcc growth, two stacking sequences (ABCABC... and ACBACB...) generated by twinning on the (111) mirror planes are possible. In fact, Ag nucleates as islands on GaAs (111) with equal distribution of these two twin related domains. These grains subsequently propagate into the multilayer stacks and account for the single crystal electron diffraction patterns. Superposition of such grains in a cross-sectional view lead to Moire fringes with a spatial frequency of  $0.149 \text{ \AA}^{-1}$  as observed in the optical diffractograms [4]. Use of either GaAs

offcut by a few degrees from the exact (111) orientations or single crystal Ag should selectively nucleate only one of the two twin variants. These type of samples are currently being synthesized.

3. *Double positioning and related growth modes:* In-situ RHEED and LEED experiments during growth show six fold symmetry (figure 2). For fcc structures, double positioning at two different sites (A & B) in the (111) growth planes are possible. Grains generated by nucleation on the two sites are rotated by  $180^\circ$  about the film normal. In addition to accounting for the six-fold symmetry, when combined with twinning this double positioning gives rise to four different possibilities. Boundaries between these four types of grains are incoherent.[5].

4. *Stability of FCC structures of Co:* Earlier measurements have suggested that the fcc form of Co reverts to the more stable hcp structure

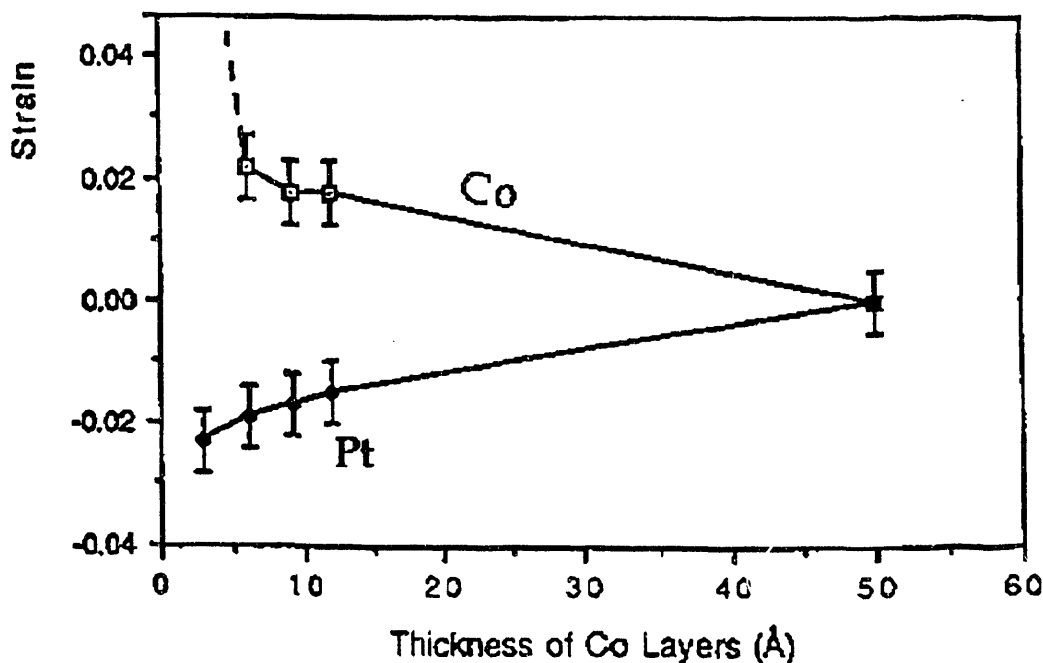


Figure 3: In-plane lattice strain measured by the position/splitting of the (220) spots for the various components of the multilayer stack. The reflections from the GaAs substrate were used to calibrate the diffraction patterns and obtain a quantitative measurement of the strain. By careful measurements of plan view as well as cross-section samples it was determined that the lattice strain was in-plane.

for  $x \geq 20 \text{ \AA}$ . However, by careful scattering measurements using both electron and photon beams, in a variety of geometries (grazing incidence, plan-view transmission, cross-section transmission) we have convincingly demonstrated that the Co fcc structure persists upto  $x = 50 \text{ \AA}$  [5].

5. *Interface mixing and compound formation* : For  $x=3, y=15, n=15$ , transverse x-ray scans through the low angle multilayer Bragg peaks show the interfaces to be diffuse in nature indicative of considerable in-plane inhomogeneity and/or compound formation. High resolution electron microscopy measurements of cross-sections (figure 2) compared with image

simulations confirm that the interface layer is diffuse and its stoichiometry is such that the Co occupation is less than 40%. Redistribution of Co should then extend over at least four monolayers [3]. However, the exact stoichiometry or the structure of the interface layer is still unclear, given the wide range of miscibility for Co in Pt. Curie temperature measurements should provide conclusive evidence of the nature of the intermixed layer, particularly if it is ordered

6. *Strain*: There is a 10% lattice mismatch between fcc Co and Pt. Kerr rotation and electron diffraction measurements for a range of  $(\text{Co}_x\text{Pt}_y)_{15}$  samples show that the largest

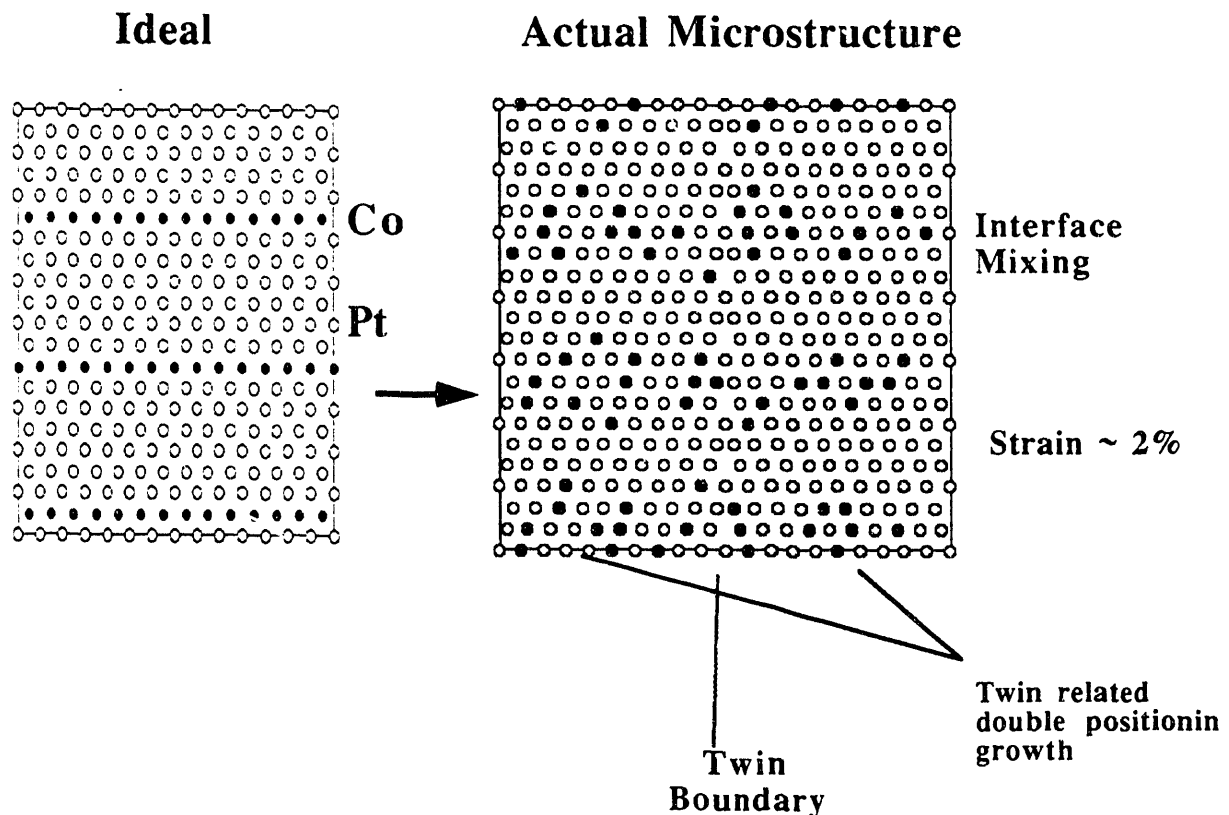


Figure 4: Models of both the ideal nanostructure and the actual microstructure that evolves during synthesis. Note that in this [110] projection, two twin related grains (and boundary) and an interface layer that is diffuse over four monolayers is shown. In addition, the Pt layers exhibit an in-plane strain of  $\sim 2\%$ .

perpendicular anisotropy and square hysteresis loop is achieved when  $x=3\text{\AA}$  and the Pt layer is subject to about 2% in-plane strain. However, along with increasing Co thickness, the Co and Pt layers lose coherency and the magnetic anisotropy goes from being perpendicular to planar. This is accompanied by a relaxation of lattice strain in both the Co and Pt layers. At  $x=y=5\text{nm}$ , the lattice parameter of both Co and Pt relax to their bulk values along with an absence of perpendicular anisotropy. These measurements underscore the importance of magneto-elastic anisotropy due to lattice mismatch between the adjacent epitaxial layers.[6]. Once the details of these microstructural parameters (figure 4) are quantitatively established they can be used as inputs for micromagnetic calculations to predict the unique magnetic properties of such nanostructures.

#### IV. REFERENCES

1. L. M. Falicov et al, J. Mat. Res. **5**, 1299 (1990) .
2. Kannan M. Krishnan, Appl. Phys. Lett., **61** \_\_\_\_\_(1992)
3. N. -H. Cho, Kannan M. Krishnan, C. A. Lucas and R.F.C. Farrow, Jour. Appl. Phys., **72**, \_\_\_\_\_(1992)
4. N. -H. Cho, Kannan M. Krishnan, C. H. Lee and R.F.C. Farrow, Appl. Phys. Lett. **60**, 2371(1992)
5. B. Zhang, Kannan M. Krishnan and R.F. C. Farrow, Ultramic., in press
6. B. Zhang, Kannan M. Krishnan, C.H. Lee and R. F. C. Farrow, Jour. Appl. Phys., in press.

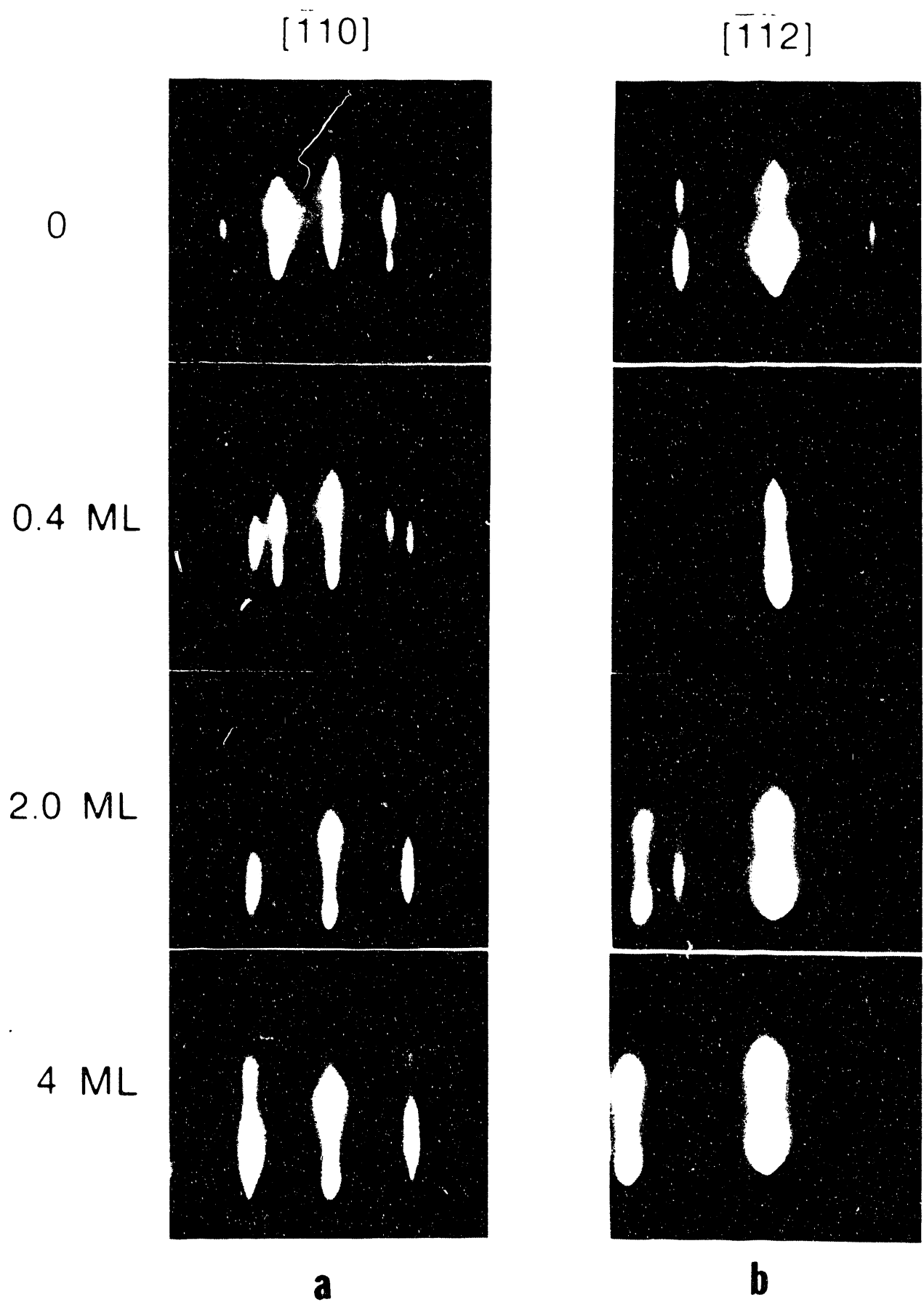


Figure 1

XBB 919-7188



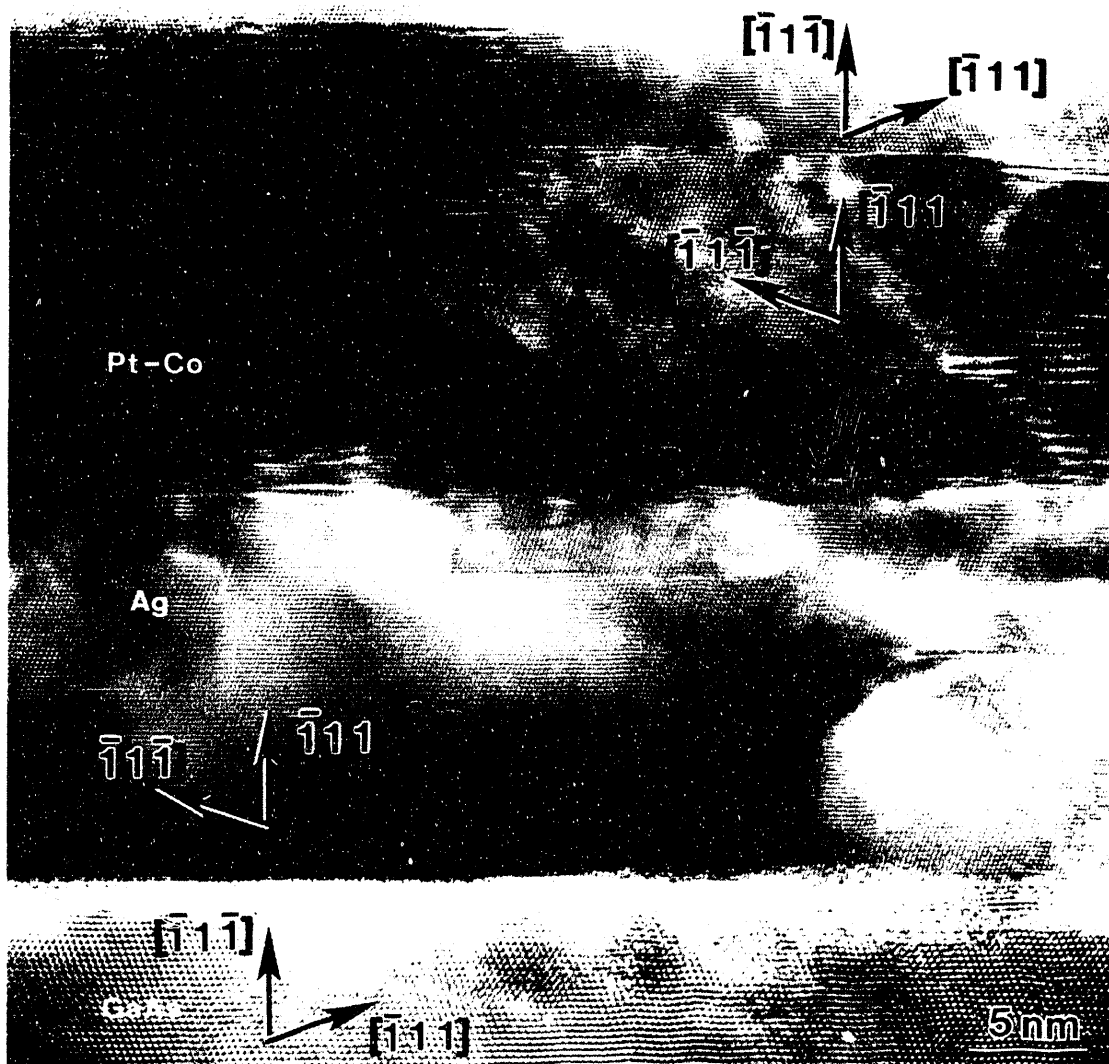
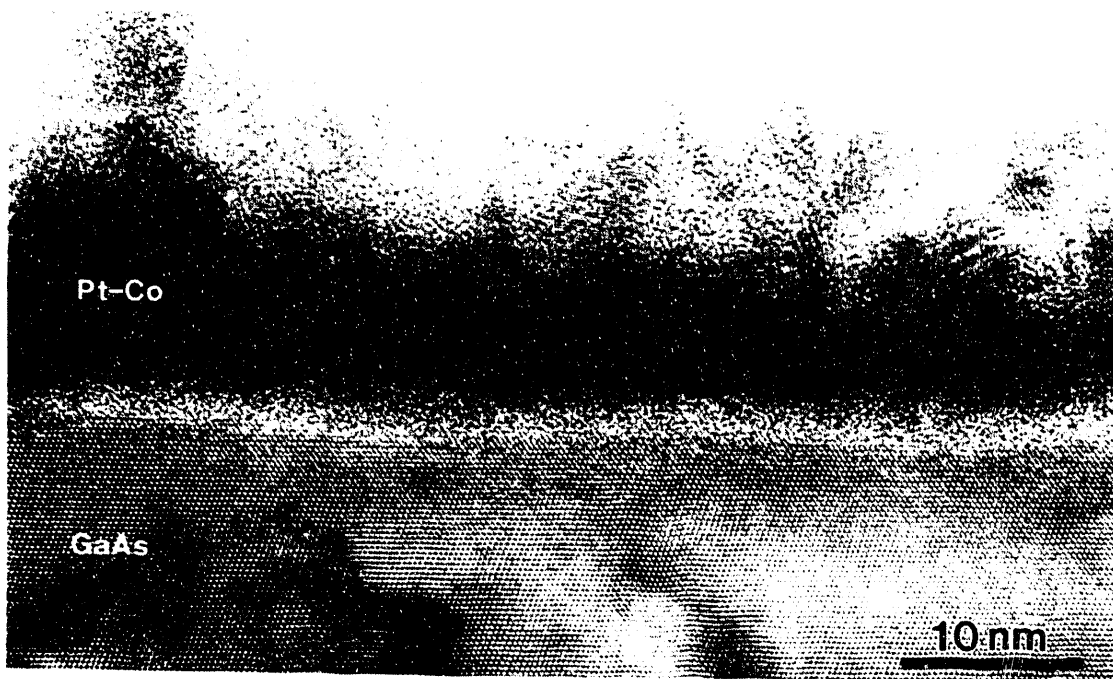


Figure 2

**END**

**DATE  
FILMED**

4 / 19 / 93

